The Astrophysical Journal, 576:L15–L18, 2002 September 1
© 2002. The American Astronomical Society. All rights reserved. Printed in U.S.A.

ITERATION METHOD TO DERIVE EXACT ROTATION CURVES FROM POSITION-VELOCITY DIAGRAMS OF SPIRAL GALAXIES

Tsutomu Takamiya and Yoshiaki Sofue
Institute of Astronomy, University of Tokyo, 2-21-1 Osawa, Mitaka, Tokyo 181-0015, Japan; sofue@ioa.s.u-tokyo.ac.jp
Received 2002 June 5; accepted 2002 July 19; published 2002 July 30

ABSTRACT

We present an iteration method to derive exact rotation curves (RCs) of spiral galaxies from observed position-velocity (PV) diagrams that comprises the following procedure. An initial RC (RC0) is adopted from an observed PV diagram (PV0) obtained by any simple method, such as the peak-intensity method. Using this RC and an observed radial distribution of intensity (emissivity), we construct a simulated PV diagram (PV1). The difference between an RC obtained from PV1 and the original RC (e.g., difference between peak-intensity velocities) is used to correct the initial RC to obtain a corrected rotation curve, RC1. This RC1 is used to calculate another PV diagram (PV2) using the observed intensity distribution and to obtain the second iterated RC (RC2). This iteration is repeated until PV*i* converges to PV0 so that the difference between PV*i* and PV0 becomes minimal. Finally, RC*i* is adopted as the most reliable RC. We apply this method to some observed PV diagrams of nearby galaxies and show that the iteration successfully converges to give reliable RCs. We show that the method is powerful in detecting central massive objects.

Subject headings: galaxies: ISM — galaxies: kinematics and dynamics — galaxies: nuclei — galaxies: structure — ISM: kinematics and dynamics — methods: data analysis

1. INTRODUCTION

Rotation curves (RCs) are one of the most basic sources of information on the dynamics of galaxies (Sofue & Rubin 2001). RCs are used to discuss supermassive black holes (e.g., Dressler & Richstone 1988; Kormendy & Richstone 1992; Bower et al. 1998), the dark matter distribution in the halo (e.g., Rubin et al. 1985; Kent 1986; Persic, Salucci, & Stel 1996; Honma & Sofue 1997; Takamiya & Sofue 2000), the characteristics of a bulge and disk (e.g., Kormendy & Illingworth 1982; Kent 1986; Héraudeau & Simien 1997), and kinematic peculiarities (e.g., Márquez & Moles 1996; Barton, Bromley, & Geller 1999; Rubin, Waterman, & Kenney 1999).

RCs of disk galaxies are usually derived from position-velocity (PV) diagrams by optical (Hα, [N II]) and radio (CO, H I) line observations (Sofue & Rubin 2001). There have been several ways to derive RCs. Widely used methods are to trace intensity-weighted velocities (Warner, Wright, & Baldwin 1973) and to trace peak-flux ridges in PV diagrams (e.g., Rubin et al. 1985; Mathewson et al. 1992). These methods give good results for nearly face-on galaxies with sufficiently high spatial resolutions. Other methods are the terminal velocity method used for our Galaxy (e.g., Clemens 1985) and the envelope-tracing method (Sofue 1996, 1997), which traces the envelope velocities on PV diagrams and corrects for the intrinsic interstellar velocity dispersion and resolutions to estimate terminal velocities. This method gives better results for the central regions and for highly inclined and edge-on galaxies (Olling 1996). Sofue (1996, 1997) applied this method also to intermediately inclined galaxies to obtain central-to-outer RCs of many spiral galaxies. The envelope-tracing method would be the most practical way to derive RCs in disk galaxies, however it still has difficulties deriving exact velocities in the central regions because of very high apparent velocity widths due to (1) unresolved, rapidly rotating components whose radial and tangential points are observed in a finite beam, (2) steep velocity gradients, and (3) complex gas distribution.

In this Letter we first analyze the observational conditions under which the peak-traced velocity does not accurately follow the true rotation velocity by simulating PV diagrams using model RCs. Next, we propose a new iteration method to derive an RC, and we apply it to some observations and compare it with the peak-flux and envelope-tracing methods. We finally stress the advantages of using the iteration method to search for central massive cores and black holes.

2. POSITION-VELOCITY DIAGRAM SIMULATION

Given an RC, the shape of a PV diagram depends on the observational parameters, such as the seeing size, slit width, or equivalently the beam size, and spectral resolution. The PV shape also depends on the intrinsic parameters of the galaxy itself, such as the inclination of the disk, interstellar velocity dispersion, and gas distribution. In order to see how these parameters affect the observed PV diagrams, we simulate PV diagrams from a given RC for a model galaxy and show the results in Figure 1. Observational parameters, such as the assumed slit width, velocity resolution, and seeing size, are given across the top of the figure.

The model galaxy is put at a distance of 10 Mpc ($1'' = 49$ pc). The galaxy is assumed to have a similar RC as the Milky Way, expressed by a Miyamoto-Nagai potential model (Miyamoto & Nagai 1975) with a massive central core, bulge, disk, and dark halo, as shown by the thick line in the upper panel. The gas disk has an exponential density profile as indicated by the thin line in the lower panel, which is expressed by

$$\rho \propto \exp\left(-\frac{r}{h_r} - \frac{|z|}{h_z}\right), \quad (1)$$

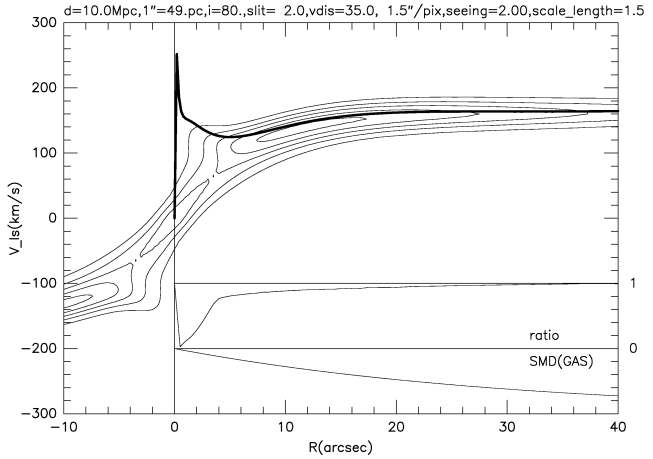

FIG. 1.—*Upper curves*: Simulated PV diagram from an assumed RC (*thick line*). *Middle curve*: Difference of the peak-traced velocity in the PV diagram from the original RC. *Lower curve*: Gas density distribution used for constructing the PV diagram.

where r, z, h_r, and h_z are the radius, height from the galactic plane, scale radius, and scale height, respectively. We assume that $h_r = 1.5$ kpc and $h_z = 60$ pc and that the inclination is 80°. The interstellar velocity dispersion on the order of 5–10 km s^{-1} is assumed to be sufficiently small compared to the observational velocity resolution, which is taken to be 35 km s^{-1}.

The middle curve of Figure 1 shows the ratio of the "observed" peak-intensity velocity in the simulated PV diagram to the assumed rotation velocity. The simulated PV diagram behaves like a rigid body in the central regions, and hence, if we use peak-intensity velocities, the rotation velocity is significantly underestimated. We also made the simulation for various parameter sets and found that the larger the inclination, the greater the underestimate of the rotation velocity because we observe more foreground and background disk gases on the line of sight with nearly zero radial velocities for higher inclination galaxies.

Moreover, if the central region is gas deficient, namely, if the gas distribution is ringlike, the observed PV diagram behaves more rigid-body–like, even if the assumed central rotation velocity was extremely high. Underestimation of central rotation velocities was found in all cases, and it amounted to 50%–100% of the intrinsic rotation velocities. Underestimates were found even using the envelope-tracing method, although it gave better results than the peak-tracing method. Hence, the current widely used methods may not be appropriate to discuss RCs and related properties, such as the mass distribution in the central regions of spiral galaxies.

3. ITERATION METHOD

In order to derive more reliable RCs from observed PV diagrams, particularly for the central regions of spiral galaxies, we propose a new method that comprises the following algorithm, which we call hereafter the iteration method. Figure 2 shows the flow chart of this algorithm:

1. We define a radial velocity profile traced at a 20% level envelope of the peak flux in a PV diagram as a comparison velocity and take this profile as the initial trial RC, $V_{\rm ini}(r)$.

2. At each radius we calculate velocity-integrated intensity using the observed spectrum, or equivalently by integrating the PV diagram in the direction of velocity at a fixed radius. We assume that the integrated intensity is proportional to the column density of interstellar gas along the line of sight, $\Sigma(r)$. The gas density distribution, $\rho(r, z)$, in the galaxy is assumed to have a disk form with an exponential z-directional structure:

$$\rho(r, z) = A\Sigma(r) \exp\left(-\frac{|z|}{h_z}\right). \quad (2)$$

Here $h_z = 100$ is the scale height of the disk and is assumed to be constant at 100 pc for all galaxies. The constant coefficient A is taken to be arbitrary because the absolute values of PV intensities do not affect the resultant rotation velocities in the present method. The thus calculated $\rho(r, z)$ is used through the entire iteration process.

3. Based on $V_{\rm ini}(r)$ and $\rho(r, z)$, a PV diagram is calculated using observational parameters, such as the slit width, velocity resolution, and seeing size (beam size), which are taken to mimic the real observations. We use this new PV diagram to derive a new 20% level envelope of the peak flux, and we obtain a new RC with velocities $V_{\rm com}$.

4. We define the difference between the first trial RC and this calculated RC by $\delta V = V_{\rm ini} - V_{\rm com}$ and use it to correct for $V_{\rm ini}$ to obtain the second iterated RC, $V_2 = V_{\rm ini} + \delta V$.

5. We calculate another PV diagram using V_2 and obtain the second iterated RC, $V_{\rm com,\,2}$, which is then compared with $V_{\rm ini}$ to calculate $\delta V_2 = V_{\rm ini} - V_{\rm com,\,2}$, and we obtain $V_3 = V_2 + \delta V_2$.

6. We repeat this procedure for i times to obtain the ith iterated RC, $V_i = V_{i-1} + \delta V_i$, until δV_i becomes smaller than a criterion, i.e., until $|\delta V_i|$ becomes sufficiently small compared to the velocity resolution. Here $V_{\rm com,\,i}$ converges to $V_{\rm ini}$ within the error, and the calculated RC becomes approximately identical to the observed RC within the rms noise. Finally, we adopt V_i as the most reliable RC.

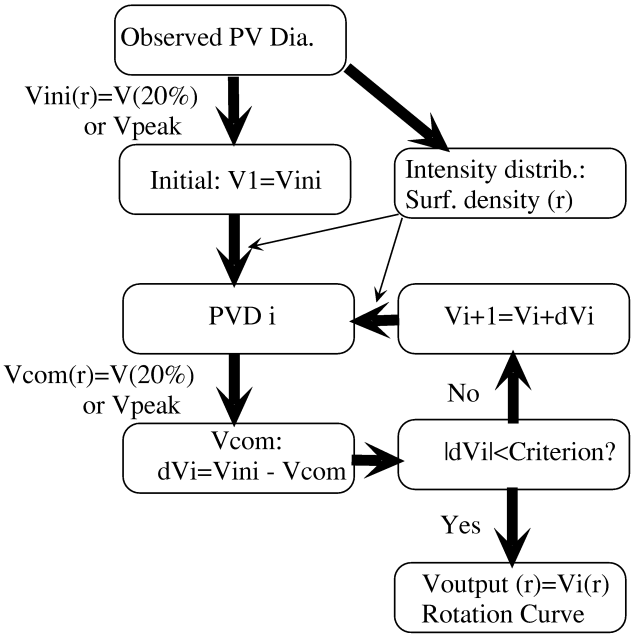

FIG. 2.—Flow chart of the algorithm of the iteration method to derive an RC from the observed PV diagram.

Here we used the original Σ obtained from observation to calculate the iterated PV diagrams, although we used corrected velocities. In order to obtain fully consistent iteration, the surface density must also be replaced by corrected values. How-

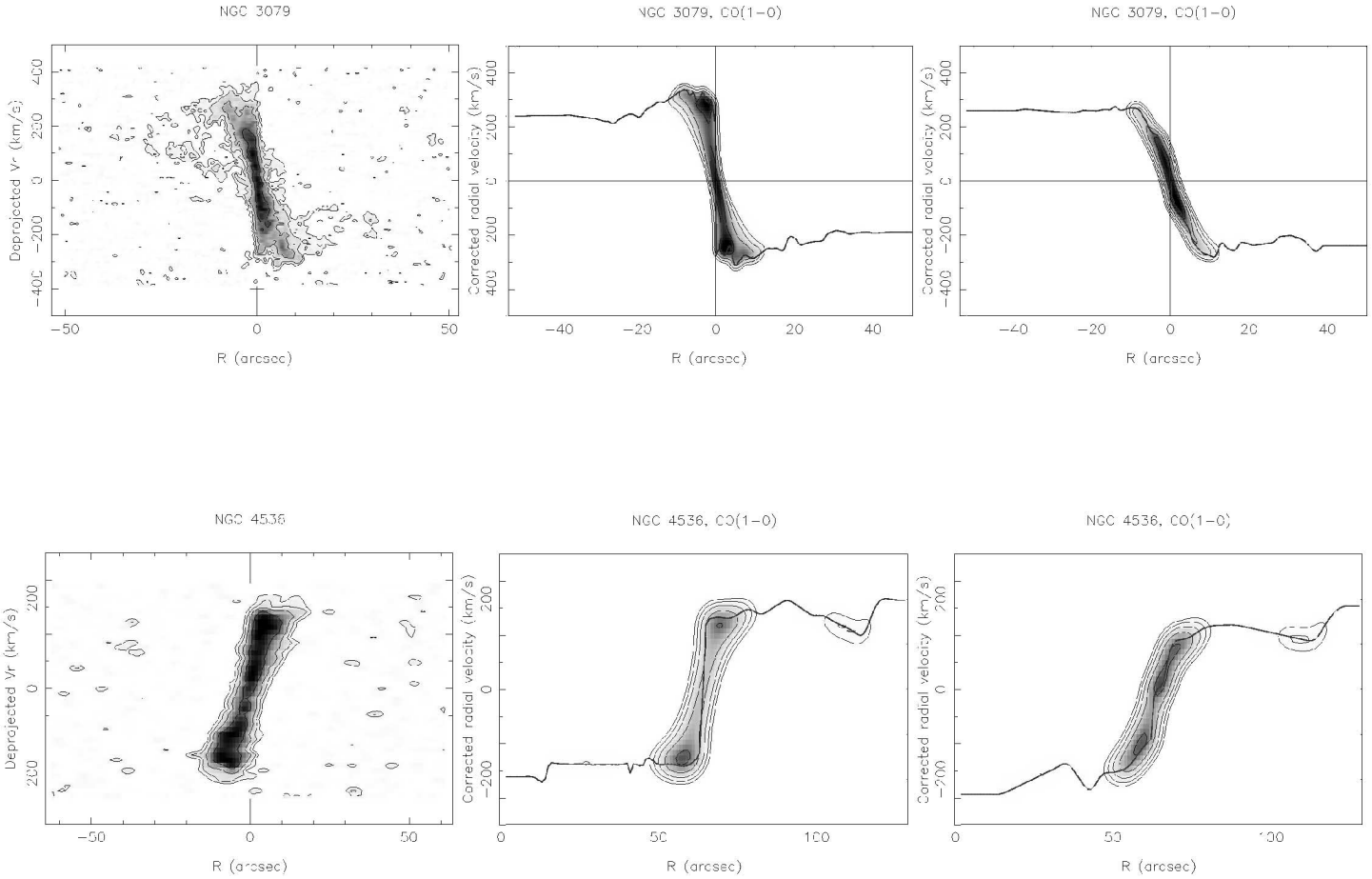

FIG. 3.—*Upper left panel*: Observed PV diagram of the edge-on galaxy NGC 3079. *Upper middle panel*: RC obtained by the iteration method and the resultant PV diagram. *Upper right panel*: Peak-traced rotation velocity and corresponding PV diagram. *Lower panels*: Same as upper panels, but for the Sb galaxy NGC 4536.

ever, this would make the program very sophisticated, and it will be a subject for the future. We mention only that the correction for Σ would be much less effective compared to the correction to velocities because the gas distribution is not expected to change so drastically compared to velocities, which may have an extremely steep rise near the nucleus.

4. APPLICATION TO OBSERVATIONAL DATA

We applied the iteration method to optical spectral data obtained by using the 1.88 m telescope at the Okayama Astrophysical Observatory (Sofue et al. 1999) and to the CO ($J = 1 - 0$) line data observed with the Nobeyama Millimeter-wave Array (NMA; Sofue et al. 2001; Koda et al. 2002; Y. Sofue et al. 2002, in preparation). Here we display some examples of the results applied to NMA CO line observations.

Figure 3, upper left panel, shows an original PV diagram for the edge-on Sc galaxy NGC 3079 in the CO line emission, exhibiting a central high-velocity rotating molecular disk. Figure 3, upper middle panel, shows the obtained RC by applying the iteration method and a constructed PV diagram by conniving this RC with the observed intensity profile. In Figure 3, upper right panel, we show a simple RC obtained by the peak-tracing method, which corresponds to the initial trial RC in Figure 2, and a convoluted PV diagram. The iteration method gives an extremely steep RC and reproduces the observed PV diagram very well. On the other hand, the peak-tracing method gives a mild RC, but the reconstructed PV diagram cannot reproduce the observation.

The lower panels in Figure 3 are the same, but applied to the mildly inclined Sb galaxy NGC 4536. Again we find the iteration method gives a reasonable reproduction of the observed PV diagram, while the other method cannot reproduce the observation. In both cases, peak-intensity velocities lead to underestimated rotation velocities by 50–100 km s^{-1} in the central regions. In Figure 4 we show some more examples of RCs obtained by the iteration method superposed on the original PV diagrams. Very steeply rising RCs are obtained for most cases.

5. DISCUSSION

The iteration method has some advantage over the current methods and will be particularly powerful in determining the central RCs and, therefore, detecting massive central objects. In fact, most of the galaxies shown in Figures 3 and 4 have very high velocities near the centers, which suggest the existence of massive cores around the nuclei. Underestimation of RCs in the central region significantly affects the discussion of the central structure (Takamiya & Sofue 2000).

The iteration method uses all data points to reproduce the observed PV diagrams by simulating the observed PV diagram, and hence, the statistical errors in the results are smaller com-

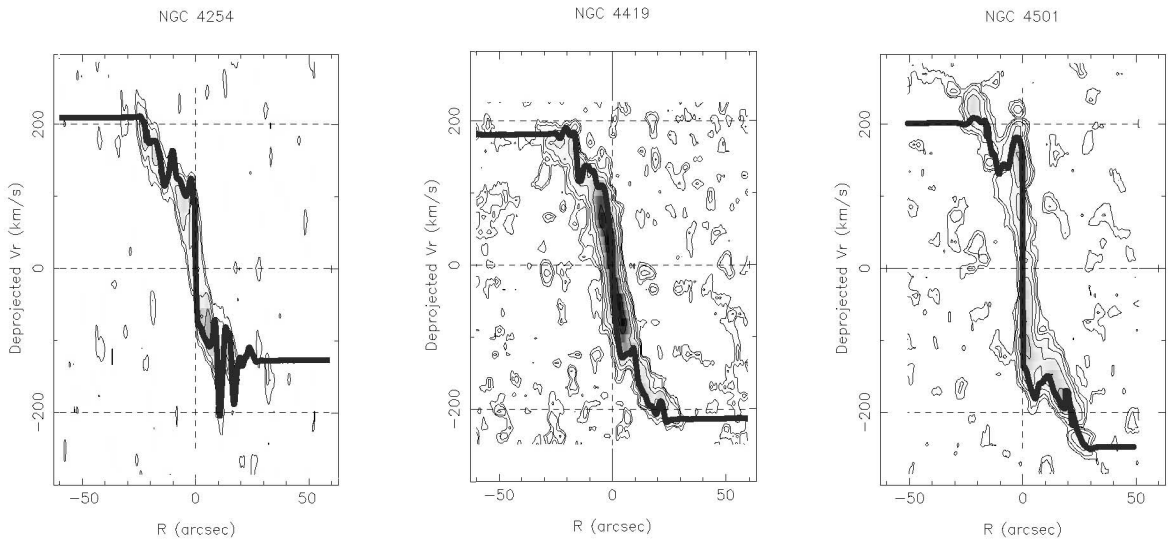

FIG. 4.—Examples of RCs obtained by the iteration method superposed on the high-resolution CO line PV diagrams obtained by the NMA (Y. Sofue et al. 2002, in preparation).

pared to those using other methods. For example, the peak-tracing and envelope-tracing methods use only a part of each velocity profile. Hence, the amount of data available to fit observation is by a factor of 10 greater in the present method than in the peak- and envelope-tracing methods. The intensity-weighted velocity method uses all data but smears out the detailed velocity information, and the result is approximately the same as that from the peak-tracing method, which also significantly underestimates the central velocities.

Finally, we stress that the present method does not need any potential model, and therefore, the result is purely observational and unique. This unique RC can be further used to calculate the mass distribution directly by a deconvolution technique as described in Takamiya & Sofue (2000). A method comparing the shapes of observed and calculated PV diagrams has been used by Bertola et al. (1998) to detect central massive objects. They assumed a central potential model in order to mimic the PV diagrams, and hence, the method cannot measure the error quantitatively and the mass model may not necessarily be unique. Application of the iteration technique to these current observations would also give more reliable answers on the existence of such massive objects.

We thank J. Koda and H. Nakamishi for their help in preparing the figures.

REFERENCES

Barton, E. J., Bromley, B. C., & Geller, M. J. 1999, ApJ, 511, L25
Bertola, F., Cappellari, M., Funes, J. G., Corsini, E. M., Pizzella, A., & Beltran, J. C. V. 1998, ApJ, 509, L93
Bower, G. A., et al. 1998, ApJ, 492, L111
Clemens, D. P. 1985, ApJ, 295, 422
Dressler, A., & Richstone, D. O. 1988, ApJ, 324, 701
Héraudeau, Ph., & Simien, F. 1997, A&A, 326, 897
Honma, M., & Sofue, Y. 1997, PASJ, 49, 453
Kent, S. M. 1986, AJ, 91, 1301
Koda, K., Sofue, Y., Kohno, K., Nakanishi, H., Onodera, S., Okumura, S. K., & Irwin, J. A. 2002, ApJ, 573, 105
Kormendy, J., & Illingworth, G. 1982, ApJ, 256, 460
Kormendy, J., & Richstone, D. 1992, ApJ, 393, 559
Márquez, I., & Moles, M. 1996, A&AS, 120, 1
Mathewson, D. S., Ford, V. L., & Buchhorn, M. 1992, ApJS, 81, 413
Miyamoto, M., & Nagai, R. 1975, PASJ, 27, 533
Olling, R. P. 1996, AJ, 112, 457
Persic, M., Salucci, P., & Stel, F. 1996, MNRAS, 281, 27
Rubin, V. C., Burstein, D., Ford, W. K., & Thonnard, N. 1985, ApJ, 289, 81
Rubin, V. C., Waterman, A. H., & Kenney, J. D. P. 1999, AJ, 118, 236
Sofue, Y. 1996, ApJ, 458, 120
———. 1997, PASJ, 49, 17
Sofue, Y., Koda, J., Kohno, K., Okumura, S. K., Honma, M., Kawamura, A., & Irwin, J. A. 2001, ApJ, 547, L115
Sofue, Y., & Rubin, V. C. 2001, ARA&A, 39, 137
Sofue, Y., Tutui, Y., Honma, M., Tomita, A., Takamiya, T., Koda, J., & Takeda, Y. 1999, ApJ, 523, 136
Takamiya, T., & Sofue, Y. 2000, ApJ, 534, 670
Warner, P. J., Wright, M. C. H., & Baldwin, J. E. 1973, MNRAS, 163, 163